

The Impact of the Extreme Winter 2015/16 Arctic Cyclone on the Barents–Kara Seas

LINETTE N. BOISVERT AND ALEK A. PETTY

Earth System Science Interdisciplinary Center, University of Maryland, College Park, College Park, and National Aeronautics and Space Administration, Goddard Space Flight Center, Greenbelt, Maryland

JULIENNE C. STROEVE

National Snow and Ice Data Center, Cooperative Institute for Research in Environmental Sciences, University of Colorado Boulder, Boulder, Colorado, and Centre for Polar Observation and Modelling, University College London, London, United Kingdom

(Manuscript received 21 June 2016, in final form 16 August 2016)

ABSTRACT

Atmospheric data from the Atmospheric Infrared Sounder (AIRS) were used to study an extreme warm and humid air mass transported over the Barents–Kara Seas region by an Arctic cyclone at the end of December 2015. Temperature and humidity in the region was $\sim 10^{\circ}\text{C}$ ($>3\sigma$ above the 2003–14 mean) warmer and $\sim 1.4\text{ g kg}^{-1}$ ($>4\sigma$ above the 2003–14 mean) wetter than normal during the peak of this event. This anomalous air mass resulted in a large and positive flux of energy into the surface via the residual of the surface energy balance (SEB), compared to the weakly negative SEB from the surface to the atmosphere expected for that time of year. The magnitude of the downwelling longwave radiation during the event was unprecedented compared to all other events detected by AIRS in December/January since 2003. An approximate budget scaling suggests that this anomalous SEB could have resulted in up to 10 cm of ice melt. Thinning of the ice pack in the region was supported by remotely sensed and modeled estimates of ice thickness change. Understanding the impact of this anomalous air mass on a thinner, weakened sea ice state is imperative for understanding future sea ice–atmosphere interactions in a warming Arctic.

1. Introduction

The 2015/16 December–February period was the warmest winter since 1880 (<http://www.ncdc.noaa.gov/sotc/summary-info/global/201602>) with surface temperature anomalies from NASA's Goddard Institute for Space Studies Surface Temperature Analysis (GISSTEMP) suggesting much of this warming occurred within the Arctic region (http://www.giss.nasa.gov/research/features/201603_gistemp/). It is well documented that the Arctic

has warmed faster than the global average over recent decades; a phenomenon known as Arctic amplification (e.g., Serreze et al. 2009; Screen and Simmonds 2010; Cohen et al. 2014). Accompanying this warming has been rapid declines in Arctic sea ice extent and thickness (e.g., Stroeve et al. 2012; Lindsay and Schweiger 2015; Serreze and Stroeve 2015; Kwok 2015). In 2016, Arctic sea ice experienced the lowest January, February, and maximum extent recorded since 1979 (<http://nsidc.org/arcticseaicenews/2016/03/another-record-low-for-arctic-sea-ice-maximum-winter-extent/>). These record low ice conditions were largely driven by anomalous low ice conditions in the Barents and Kara Seas, a region that drives most of the pan-Arctic winter sea ice variability (Fig. 1a).

In winter, cyclones are thought to be the main transporter of heat and moisture into the Arctic (Sorteberg and Walsh 2008), and could, therefore, contribute to sea ice melt in the absence of solar radiation. The changing magnitude and frequency of winter cyclone events in the

Supplemental information related to this paper is available at the Journals Online website: <http://dx.doi.org/10.1175/MWR-D-16-0234.s1>.

Corresponding author address: Linette N. Boisvert, Earth System Science Interdisciplinary Center, University of Maryland, College Park, 5825 University Research Ct. 4001, College Park, MD 20740.
E-mail: linette.n.boisvert@nasa.gov

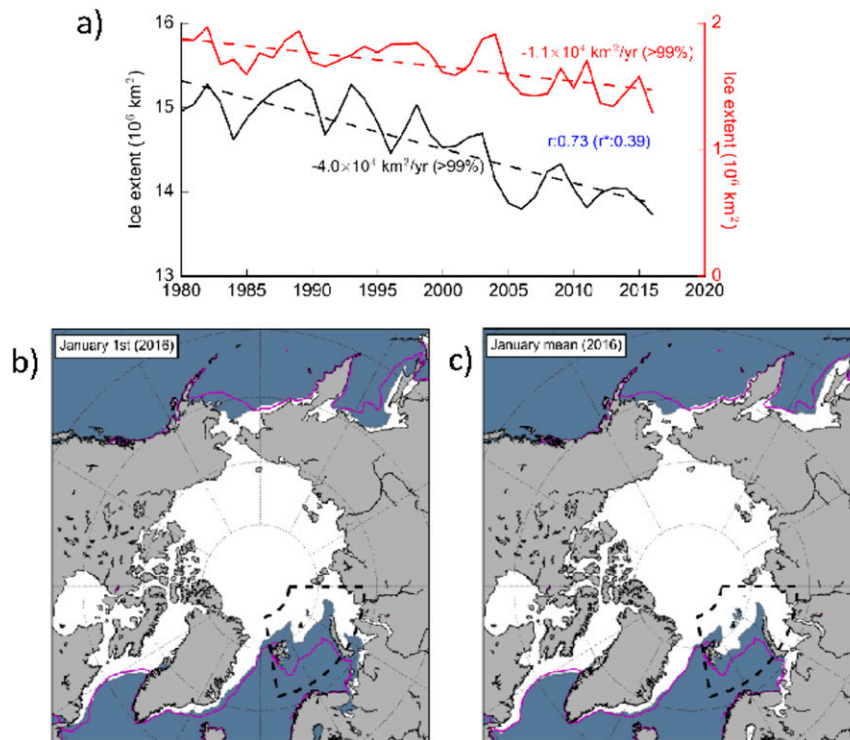


FIG. 1. (a) Mean January sea ice extent 1980–2016, in the Arctic (black line) and Barents–Kara Seas (BaKa) region (red line). Corresponding colored values are the linear trends of sea ice extent and the numbers in blue represent the correlation between the sea ice extent in the BaKa region versus the entire Arctic. (b),(c) The BaKa region is given by the dashed black box. (b) Sea ice extent for 1 Jan 2016 and (c) sea ice extent for January 2016 (monthly mean of daily extent). The magenta line in (b) and (c) indicates the median sea ice extent for 1981–2010.

Arctic remains uncertain, however, with some studies suggesting increased activity (Sorteberg and Walsh 2008; Simmonds et al. 2008; Bengtsson et al. 2006) and others suggesting no trends (Gitelman et al. 1997; Stephenson and Held 1993; Komayo et al. 2016, manuscript submitted to *J. Climate*). Late December 2015, the National Centers for Environmental Prediction (NCEP) Global Forecast System (GFS) measured above-freezing temperatures around the North Pole, driven by a strong Arctic cyclone that transported anomalously warm air from lower latitudes. The impact of this cyclone, together with the record warm winter, low sea ice extent, and the uncertainty surrounding the impact of winter cyclones on Arctic climate, warrant a more detailed examination. Here we investigate the atmosphere–surface forcing in the Barents–Kara Seas (BaKa) region (as shown in Fig. 1b) before, during, and after the cyclone (28 December 2015–4 January 2016).

2. Data and methods

a. Atmospheric data

Atmospheric data are taken from NASA’s Atmospheric Infrared Sounder (AIRS) instrument. AIRS

version 6 level 3 data products (AIRS Science Team/J. Teixeira 2013; Susskind et al. 2014) are processed within 2 days of the data being collected, making them ideal for studying near-real-time (NRT) weather events. We use daily cloud fraction, surface pressure, near-surface air temperature, and specific humidity (see text S1 in the online supplemental material) along with 8-day skin temperature data products between 2003 and 2016 (December and January).

Hourly near-surface (10 m) wind speeds are taken from the Modern-Era Retrospective Analysis for Research and Applications, version 2 (MERRA-2) reanalysis (Rienecker et al. 2011), which are then averaged daily.

b. Sea ice data

The satellite passive microwave record provides estimates of Arctic sea ice concentration (SIC) from October 1978 to 2015 derived from the NASA Team sea ice algorithm (Cavalieri et al. 1996) and NRT daily data for the 2015/16 winter (Maslanik et al. 1999).

Sea ice drift estimates are produced by the Centre ERS d’Archivage et de Traitement (CERSAT)/Institut Français de Recherche pour l’Exploitation de la Mer

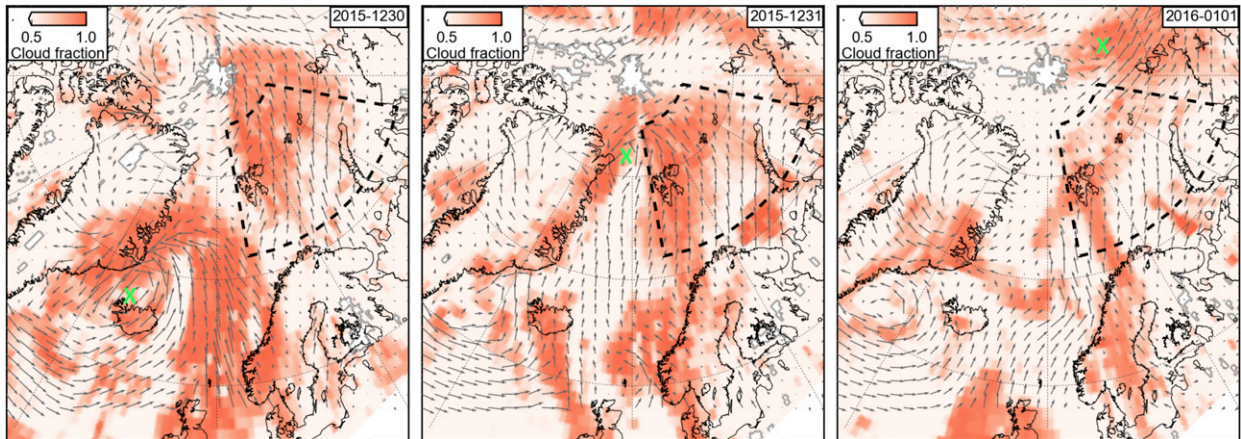


FIG. 2. MERRA-2 winds (vectors) and AIRS cloud fraction for 30 Dec 2015–1 Jan 2016, during the height of the cyclone. The center of the cyclone is designated by the green “×” in each image.

(IFREMER) (Girard-Ardhiu and Ezraty 2012). Here we use the NRT daily drift data produced through the merging of both horizontal and vertical polarizations of the Advanced Microwave Scanning Radiometer (AMSR2) (see details in text S2 in the online supplemental material).

c. Surface energy balance

Using data from AIRS and MERRA-2, we solve for all terms in the surface energy balance (SEB) (text S3 in the online supplemental material provides more detail):

$$F_r + F_L - F_E + F_s + F_e = \text{SEB}, \quad (1)$$

where F_r is the net shortwave radiation, F_L is the downwelling longwave radiation (LWD), F_E is the emitted longwave radiation, and F_s and F_e are the sensible and latent heat fluxes, respectively.

3. Results and discussion

Figure 2 shows the location of the cyclone center and hourly wind vectors (midday) from MERRA-2 overlaid on the daily AIRS cloud fraction. This cyclone formed on 28 December 2015 (990 hPa) in the middle of the North Atlantic (43°N). It then traveled northeast toward the United Kingdom as the pressure slowly dropped. On 29 December (960 hPa) it turned northwest toward Iceland, rapidly intensifying on 30 December (930 hPa). It then moved northward along the coast of Greenland into the central Arctic near 90°N on 31 December (970 hPa), where it weakened slightly. On 1 January (975 hPa), the cyclone moved to the north of Severnaya Zemlya Island. During this time a warm, moist, southerly air mass was transported over the BaKa

region. Figure S2 (in the online supplemental material) demonstrates the northeastern progression of the anomalous warm (above freezing) and moist air mass by the cyclone, from the East Greenland Sea on 28 December, which extended into the BaKa region on 30 December and lingered for several days after. Figure 3 shows the daily near-surface air temperature and specific humidity anomalies (compared to the 2003–14 mean) during the period of the storm (28 December 2015–4 January 2016), where temperatures experienced in the BaKa were, in places, up to $\sim 20^\circ\text{C}$ ($>6\sigma$) and $\sim 3 \text{ g kg}^{-1}$ ($\sim 9\sigma$) above average (2003–14) for that time of year. During the peak of this cyclone (30 December 2015–1 January 2016), the mean BaKa air temperatures were $\sim 10^\circ\text{C}$ ($>3\sigma$) warmer and the specific humidity was $\sim 1.4 \text{ g kg}^{-1}$ ($>4\sigma$) higher than the 2003–14 average (see Fig. S1 in the online supplemental material). Atmospheric anomalies over the BaKa region remained higher than average from 2 to 6 January [a mean of 6.6°C ($>2\sigma$) and 0.5 g kg^{-1} ($>1\sigma$), Fig. 3]. Before the cyclone entered the Arctic (15–27 December 2015), the BaKa air temperature and humidity was only slightly warmer [$\sim 0.8^\circ\text{C}$ ($<1\sigma$)] and $\sim 0.2 \text{ g kg}^{-1}$ ($<1\sigma$) more humid than the 2003–2014 mean (not shown), suggesting this cyclone had a large impact on the SEB in the region.

a. Surface energy budget during the cyclone

Figure 4 (top) shows daily maps of the SEB from 28 December 2015 to 4 January 2016. Over most of the Arctic the SEB is small, dominated by the upwelling longwave heat flux and LWD opposing each other. The turbulent heat fluxes are predominantly negligible through winter (based on climatology), except in the North Atlantic where the warm ocean surface loses heat and moisture to the cold atmosphere (a negative SEB

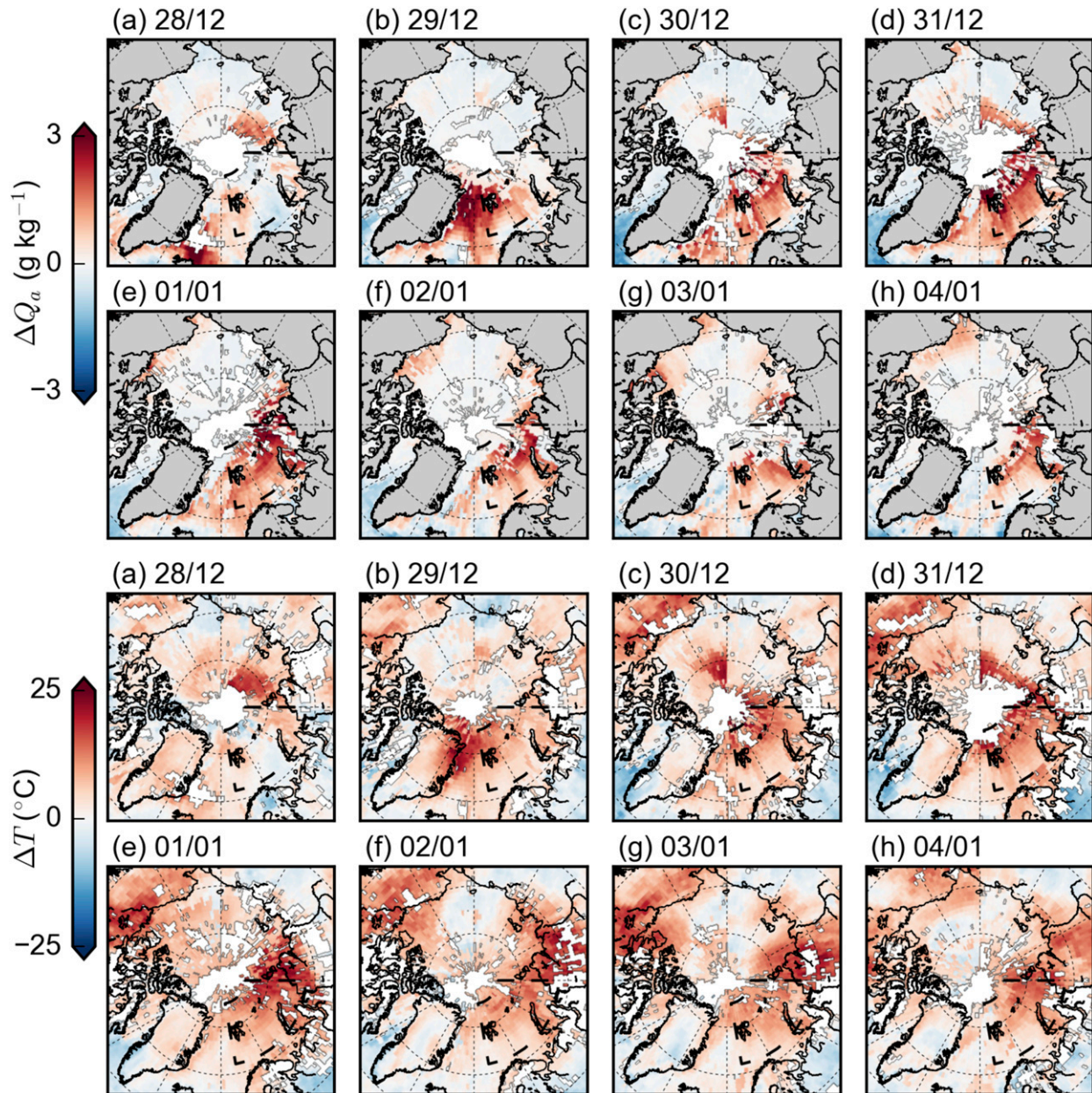


FIG. 3. (top) Near-surface specific humidity anomalies and (bottom) near-surface temperature anomalies from 28 Dec 2015 to 4 Jan 2016, compared to the 2003–14 mean. Red temperatures signify positive anomalies. White areas have no data. The BaKa region is highlighted by the black dashed boxes.

contribution). Before the cyclone transported this air mass into the BaKa region (~ 28 December), the SEB was negative (i.e., the ocean surface was losing energy to the atmosphere), favoring ice formation/growth. After the air mass entered the BaKa region, the SEB became positive (i.e., the surface was gaining energy from the atmosphere).

Figure 4 (bottom) shows the daily mean SEB for the BaKa region during the cyclone and for the 2003–14 mean. From 30 December 2015 to 1 January 2016, the

SEB was positive instead of negative, and was roughly the same magnitude, but in the opposite direction compared to the 2003–14 mean ($\sim 45 \text{ W m}^{-2}$). The daily SEB peaked on 31 December 2015, dominated by increases in sensible heat ($\sim 60 \text{ W m}^{-2}$ increase), followed by LWD ($\sim 50 \text{ W m}^{-2}$ increase) and latent heat ($\sim 20 \text{ W m}^{-2}$ increase).

Figure 4 (bottom) additionally shows values for the SEB over the BaKa sea ice areas only ($>50\%$ SIC,

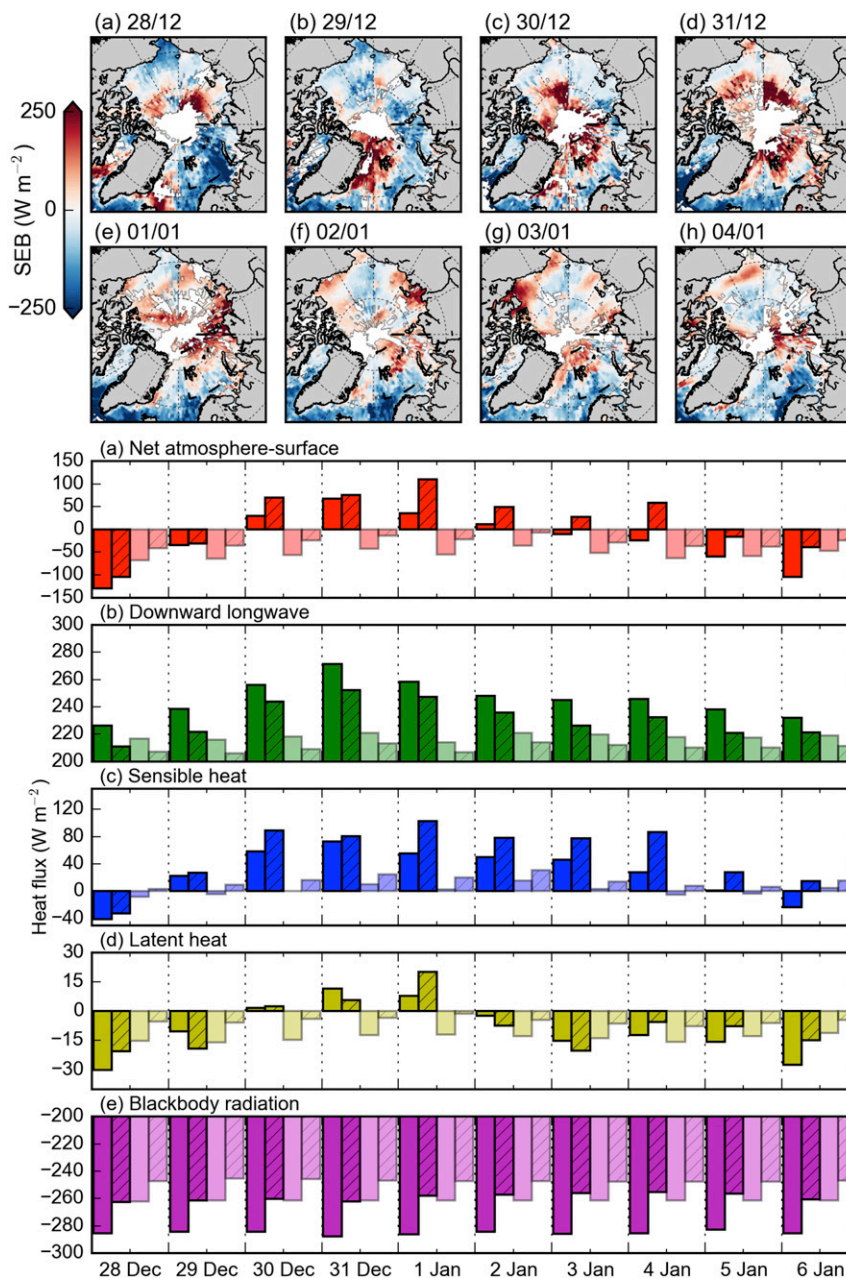


FIG. 4. (top) Surface energy balance over the Arctic from 28 Dec 2015 to 4 Jan 2016. The data over land have been masked. (bottom) Net surface energy balance and respective terms from 28 Dec 2015 to 6 Jan 2016 (solid bars) and for the 2003–14 mean (light shaded bars). Hatched bars (both solid and light shaded) represent the net surface energy balance over sea ice (>50% ice concentration). Values shown for all variables are for the BaKa region.

hatched bars). Compared to the 2003–14 mean, the SEB over the sea ice areas during the cyclone showed anomalous LWD ($\sim 40 \text{ W m}^{-2}$) and turbulent heat fluxes ($\sim 120 \text{ W m}^{-2}$) into the surface, resulting in an increase in the SEB over sea ice to $\sim 110 \text{ W m}^{-2}$.

Following this peak, the SEB declined but remained mostly positive, especially over the ice-covered areas.

The 2003–14 mean suggests the SEB normally remains negative at this time of year. The positive SEB after the cyclone was driven by stronger-than-normal LWD and sensible heat fluxes, and suggests a stalling of ice formation in the region. While the SEB for the later part of January 2016, was not a part of this study, the lack of sea ice recovery in the BaKa region (the mean January sea

ice extent shown in Figs. 1b and 1c) also suggests the surface did not lose enough heat for sea ice formation to occur, at least at amounts significant enough to be detected by the NASA Team sea ice algorithm. The effects of this increased SEB on the sea ice in the BaKa region will be discussed more in section 3b.

HOW DOES THE DECEMBER 2015 CYCLONE COMPARE TO OTHER EVENTS IN THE AIRS RECORD?

The air mass associated with this cyclone was extreme when compared to average conditions, but was this unusual when compared to other anomalous events in winter [December–January (DJ)] during the AIRS record? To detect and compare this event with other anomalous “elevated events” (that may or may not have been the result of a cyclone), we follow Park et al. (2015) and use LWD to assess the presence of an elevated event. LWD is used because normally the winter Arctic boundary layer is stable (limiting turbulent fluxes) and there is no solar radiation in DJ for the majority of the Arctic; thus the winter Arctic SEB is near zero and dominated by LWD variability (Serreze et al. 2007). Morrison et al. (2011) discussed how changes in the atmosphere from dry and clear, to moist and cloudy, could significantly alter the LWD.

In this study, an elevated event is one where the daily mean LWD in the BaKa region is greater than one standard deviation (1σ) from the 2003–15 mean (averaged over December–January) and remains higher than 1σ for three or more consecutive days. Using these criteria, 15 elevated events were found in the BaKa region since 2003 (Fig. 5). The 2015/16 event had a mean LWD of $\sim 250 \text{ W m}^{-2}$ ($\sim 2\sigma$ from the mean), which was $\sim 8 \text{ W m}^{-2}$ greater than the average of all other elevated events ($\sim 242 \text{ W m}^{-2}$) (see text S4 in the online supplemental material). The maximum LWD (31 December 2015) was the largest on record ($>3\sigma$) and was $\sim 40 \text{ W m}^{-2}$ greater than the mean of all other event maxima. Only one other elevated event was detected with a maximum LWD greater than 2σ (in January 2012). Woods and Caballero (2016) found LWD anomalies of $\sim 30 \text{ W m}^{-2}$ during winter moisture intrusion events in the central Arctic, similar to our results.

b. Exploring the sea ice response

As shown in Fig. 1, the ice extent within the BaKa region was anomalously low during the cyclone time period, and remained low for the month of January. Figure 6a shows the daily SIC in the BaKa region from 20 December to 30 January for 2003–16. Between 30 December 2015 and 6 January 2016, the SIC decreased by $\sim 10\%$ (from 40% to 30%). Similar to the conclusions from Zhang et al. (2013), it takes around

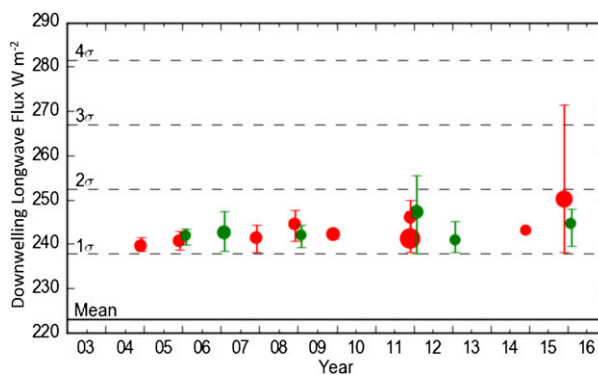


FIG. 5. Elevated downwelling longwave radiation events detected in the BaKa region for January and December, 2003–16. Events that occurred in December are in red and those that occurred in January are in green. The circles indicate the mean downwelling longwave radiation of all days during the elevated event, while the lines indicate the maximum and minimum daily downwelling longwave radiation of each elevated event. The size of the circles denotes the length of each event, with the larger the size pertaining to more days.

2 weeks (from ~ 28 December to 14 January) for the sea ice extent to return to what we might have expected from linear trend persistence. Although the SIC increased to $\sim 45\%$ during the middle of January, it decreased again (to $\sim 40\%$) toward the end of the month. Interestingly, the 2011/12 SIC showed a similar decline (albeit later, in the middle of January), which coincides with the January 2012 LWD elevated event shown in Fig. 5. The longest elevated event (12 days, late December 2011) also shows a decline in SIC, but this is weaker than the 2015/16 decline, likely due to the smaller LWD anomaly. The most pronounced SIC decline occurred during January 2006, and was attributed to unusually strong and warm southerly winds (Comiso 2006).

As Fig. 1c shows, large parts of the BaKa region remained ice free during January. Freeze-up occurred later than average over much of the Arctic in 2015 (see Fig. S3 and text S5 in the online supplemental material), but was especially noticeable in the BaKa region, where freeze-up across the northern BaKa region occurred in December (roughly 2 months later than the 2003–14 average), or not at all. We hypothesize that this late freeze-up resulted in a thinner and weaker ice pack, which was susceptible to a dynamical retreat of the ice edge. The anomalous (positive) SEB may have also resulted in surface melt during the storm, further weakening the ice pack.

Here we explore the potential dynamic/thermodynamic forcing of the observed concentration decline, but acknowledge that ocean forcing (see text S6 in the online supplemental material) is likely a significant contributor to the decline over the longer winter period.

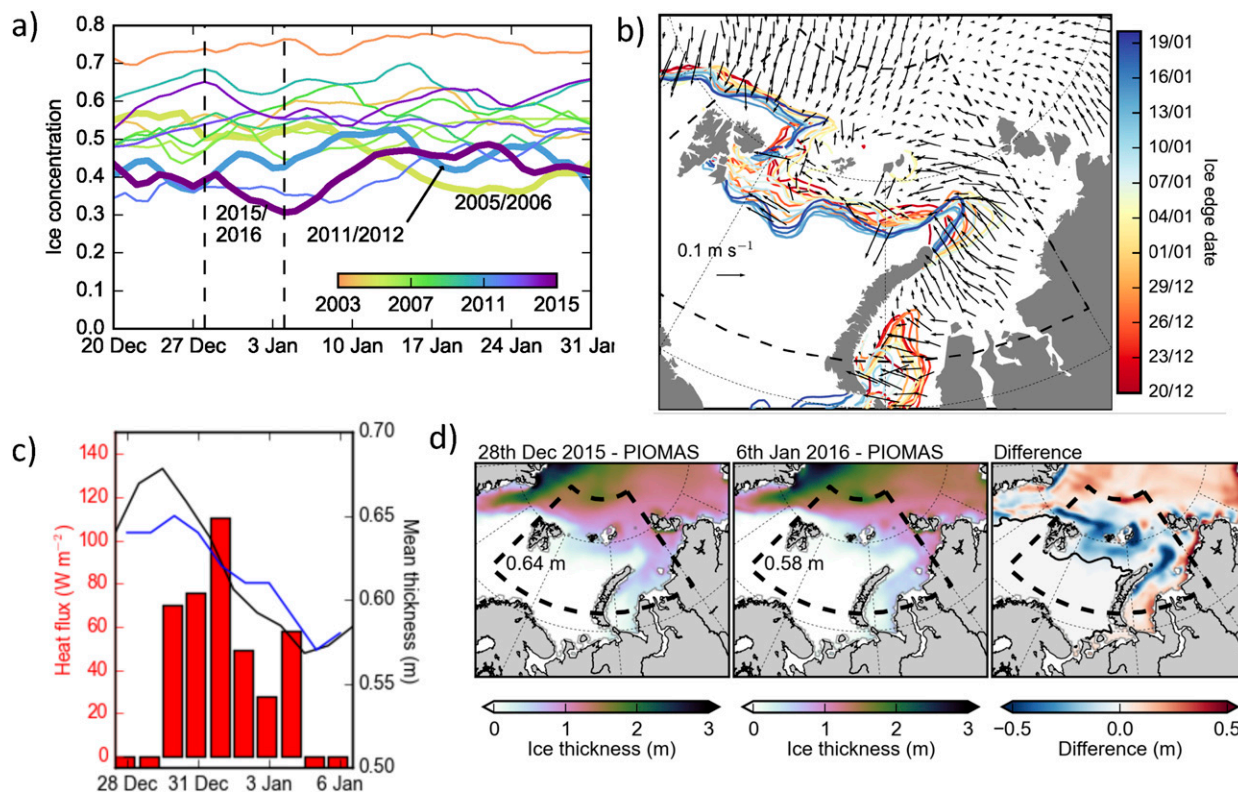


FIG. 6. (a) Daily sea ice concentration in the BaKa region from 20 Dec to 31 Jan for years 2003/04–2015/16. The bold purple (yellow/green, blue) line is the ice concentration for 2015/16 (2005/06, 2011/12). The dates of the 2015/16 event are shown by the dashed vertical lines. (b) Daily ice edge (colored lines), where the ice concentration is greater than 15%, for 20 Dec 2015–20 Jan 2016, and mean CERSAT/AMSR2 sea ice drift vectors (black arrows) over the same time period. (c) The surface energy balance over the sea ice (concentration $>50\%$) during the cyclone (red bars, 28 Dec 2015–6 Jan 2016) and the amount of melt it accounts for in the BaKa region starting out at 0.64 m (black line). The blue line is the daily thickness for the BaKa region from PIOMAS. (d) PIOMAS ice thickness maps for the BaKa region on 28 Dec 2015 and 6 Jan 2016 and the ice thickness difference between the 2 days.

1) ICE DYNAMICS

The CERSAT/AMSR2 ice drift vectors (Fig. 6b) suggest a clear cyclonic (anticlockwise) ice circulation in the BaKa region during the cyclone. The strongest ice drifts appear in the Kara Sea, transporting ice from north of Novaya Zemlya Island to the west of Severnaya Zemlya Island. Some of this ice was transported westward, toward Fram Strait, and some eastward, farther into the Kara Sea. Figure 6b shows the drift vectors overlaid on the daily ice edge during the cyclone, suggesting an eastward ice edge retreat in the eastern Barents Sea and a more variable ice edge in the western Barents Sea.

After the storm, weather conditions returned to more normal conditions for January, albeit warmer than average, with high pressure and the majority of the wind flow northerly. The high air temperature and humidity that remained in the region even after the cyclone passed (3.75 K and 0.5 g kg^{-1} , both 30% higher than the 2003–15 January average) could have hindered the ice from

recovering (cf. Figs. 1b and 1c). The anomalously low January ice extent was dominated by the low ice extent in this BaKa region (Fig. 1a), and this small retreat and lack of recovery/growth appear to be a contributor.

2) ICE THERMODYNAMICS

To explore the potential thermodynamic response of the sea ice–covered BaKa region to the estimated SEB variability during the cyclone, we employ a simple approximate scaling of budgets to estimate the resultant sea ice thickness change in the region (see text S7 in the online supplemental material). We use the mean thickness of ice in the BaKa region on 28 December 2015 ($\sim 64\text{ cm}$) from the Pan-Arctic Ice-Ocean Modeling and Assimilation System, version 2.1 (PIOMAS) to initialize the thickness change estimate and compare it with the estimated change from this more sophisticated model (Schweiger et al. 2011). Figure 6c shows that the budget scaling suggests $\sim 8\text{ cm}$ of ice melt for the 10 days of SEB forcing (28 December–6 January). While this is far from

sufficient to suggest a complete melt out of sea ice in the northern BaKa region, it does suggest the potential for melting out of the thinner sea ice toward the BaKa ice edge. The PIOMAS model estimates a mean decrease of ~ 8 cm over this same time period (Fig. 6c), while maps of the PIOMAS thickness change suggest decreases of up to 40–50 cm in some regions (Fig. 6d). The daily thickness changes/variability (Fig. 6c) estimated from the budget scaling method closely match PIOMAS, and areas where the SEB are large and positive (Fig. 4, top), are similar to those regions where PIOMAS indicates decreases in ice thickness (Fig. 6d). We further analyzed thin ice thickness estimates from ESA's Soil Moisture and Ocean Salinity (SMOS) satellite (Tian-Kunze et al. 2013) (see text S7 in the online supplemental material), which corroborates the potential regional decreases of up to 40–50 cm in some regions, as well as small regions of thickness increase (see Fig. S4 in the online supplemental material).

4. Conclusions

Daily atmospheric data from AIRS were used to study an extreme warm and humid air mass that was transported over the BaKa region by an Arctic cyclone, between late December 2015 and early January 2016. During the peak of the event, the temperature and humidity in the BaKa region was $\sim 10^{\circ}\text{C}$ ($>3\sigma$) warmer and $\sim 1.4\text{ g kg}^{-1}$ ($>4\sigma$) wetter than normal (2003–14). This air mass had a significant impact on the local SEB, contrasting starkly with the small and negative SEB expected for that time period. Since this air mass transported by this storm was unlike any recorded during the winter AIRS record, studying the effects on the SEB and its impact on the sea ice is crucial, especially considering the strong sea ice declines experienced in recent decades.

Daily SIC in the BaKa region also shows a decrease and ice drift vectors also highlight a northeastern dynamical retreat of the edge during the time period of the cyclone. A simple model of sea ice melt suggests the anomalous SEB could have also resulted in an average of ~ 10 cm of ice melt. Although this forcing appears insufficient to have caused ice to melt out across the entire BaKa region, there may have been significant amounts of localized thermodynamic ice loss. Future projections of Arctic sea ice imply continued declines in thickness over the coming decades (e.g., Holland et al. 2006), meaning the impact of similar elevated events could be significantly greater.

Acknowledgments. Linette Boisvert and Alek Petty were both funded by NASA's Operation IceBridge project

science office through ESSIC 5266970 Task 727. Julianne Stroeve was funded by NASA Grant NNX11AF44G. AIRS data can be obtained online at www.airs.jpl.nasa.gov or by directly e-mailing Linette Boisvert (linette.n.boisvert@nasa.gov). The melt season data and sea ice concentration/extent data can be found at NSIDC. The CERSAT/IFREMER drift data can be found online at <ftp://ftp.ifremer.fr/ifremer/cersat/products/gridded/psi-drift/>. MERRA-2 data can be found online at <http://gmao.gsfc.nasa.gov/reanalysis/MERRA-2/>. SMOS data can be found online at <http://icdc.zmaw.de/1/daten/cryosphere/l3c-smos-sit.html>. We thank Axel Schweiger for providing the daily PIOMAS thickness estimates used in this study. The authors thank the three anonymous reviewers for their helpful feedback. The authors would also like to thank the various bloggers, journalists, and media outlets that first brought this extreme event to our attention!

REFERENCES

- AIRS Science Team/J. Texeira, 2013: Aqua AIRS Level 3 Daily Standard Physical Retrieval (AIRS+AMSU), version 006 (AIRX3STD). NASA Goddard Earth Science Data and Information Services Center (GES DISC), accessed January 2016, doi:10.5067/AQUA/AIRS/DATA301.
- Bengtsson, L., K. I. Hodges, and E. Roeckner, 2006: Storm tracks and climate change. *J. Climate*, **19**, 3518–3543, doi:10.1175/JCLI3815.1.
- Cavalieri, D., C. Parkinson, P. Gloersen, and H. J. Zwally, 1996: Sea ice concentrations from Nimbus-7 SMMR and DMSP SSM/I-SSMIS passive microwave data, version 1 (updated 2015). NASA DAAC, National Snow and Ice Data Center, accessed January 2016, doi:10.5067/8GQ8LZQVL0VL.
- Cohen, J., and Coauthors, 2014: Recent Arctic amplification and extreme mid-latitude weather. *Nat. Geosci.*, **7**, 627–637, doi:10.1038/ngeo2234.
- Comiso, J. C., 2006: Abrupt decline in the Arctic winter sea ice cover. *Geophys. Res. Lett.*, **33**, L18504, doi:10.1029/2006GL027341.
- Girard-Arduin, F., and R. Ezraty, 2012: Enhanced Arctic sea ice drift estimation merging radiometer and scatterometer data. *IEEE Trans. Geosci. Remote Sens.*, **50**, 2639–2648, doi:10.1109/TGRS.2012.2184124.
- Gitelman, A. I., J. S. Risbey, R. E. Kass, and R. D. Rosen, 1997: Trends in the surface meridional temperature gradient. *Geophys. Res. Lett.*, **24**, 1243–1246, doi:10.1029/97GL01154.
- Holland, M. M., C. M. Bitz, and B. Tremblay, 2006: Future abrupt reductions in the summer Arctic sea ice. *Geophys. Res. Lett.*, **33**, L23503, doi:10.1029/2006GL028024.
- Kwok, R., 2015: Sea ice convergence along the Arctic coasts of Greenland and the Canadian Arctic Archipelago: Variability and extremes (1992–2014). *Geophys. Res. Lett.*, **42**, 7598–7605, doi:10.1002/2015GL065462.
- Lindsay, R., and A. Schweiger, 2015: Arctic sea ice thickness loss determined using subsurface, aircraft, and satellite observations. *Cryosphere*, **9**, 269–283, doi:10.5194/tc-9-269-2015.
- Maslanik, J., J. Stroeve, K. Knowles, W. Meier, and D. Cavalieri, 1999: Near-real-time DMSP SSMIS daily polar gridded sea ice concentrations, version 1 (updated daily). Subset used: December

- 2015–January 2016, NASA National Snow and Ice Data Center Distributed Active Archive Center, accessed January 2016, doi:10.5067/U8C09DWVX9LM.
- Morrison, H., G. de Boer, G. Feingold, J. Harrington, M. D. Shupe, and K. Sulia, 2011: Resilience of persistent mixed-phase clouds. *Nat. Geosci.*, **5**, 11–17, doi:10.1038/ngeo1332.
- Park, H.-S., S. Lee, S.-W. Son, S. B. Feldstein, and Y. Kosaka, 2015: The impact of poleward moisture and sensible heat flux on Arctic winter sea ice variability. *J. Climate*, **28**, 5030–5040, doi:10.1175/JCLI-D-15-0074.1.
- Rienecker, M. M., and Coauthors, 2011: MERRA: NASA's Modern-Era Retrospective Analysis for Research and Applications. *J. Climate*, **24**, 3624–3648, doi:10.1175/JCLI-D-11-00015.1.
- Schweiger, A., R. Lindsay, J. Zhang, M. Steele, H. Stern, and R. Kwok, 2011: Uncertainty in modeled Arctic sea ice volume. *J. Geophys. Res.*, **116**, C00D06, doi:10.1029/2011JC007084.
- Screen, J. A., and I. Simmonds, 2010: Increasing fall-winter energy loss from the Arctic Ocean and its role in Arctic temperature amplification. *Geophys. Res. Lett.*, **37**, L16707, doi:10.1029/2010GL044136.
- Serreze, M. C., and J. Stroeve, 2015: Arctic sea ice trends, variability and implications for seasonal ice forecasting. *Philos. Trans. Roy. Soc. A*, **373**, 2045, doi:10.1098/rsta.2014.0159.
- , A. P. Barrett, A. G. Slater, M. Steele, J. Zhang, and K. E. Trenberth, 2007: The large-scale energy budget of the Arctic. *J. Geophys. Res.*, **112**, D11122, doi:10.1029/2006JD008230.
- , —, J. C. Stroeve, D. N. Kindig, and M. M. Holland, 2009: The emergence of surface-based Arctic amplification. *Cryosphere*, **3**, 11–19, doi:10.5194/tc-3-11-2009.
- Simmonds, I., C. Burke, and K. Keay, 2008: Arctic climate change as manifest in cyclone behavior. *J. Climate*, **21**, 5777–5796, doi:10.1175/2008JCLI2366.1.
- Sorteberg, A., and J. Walsh, 2008: Seasonal cyclone variability at 70°N and its impact on moisture transport into the Arctic. *Tellus*, **60A**, 570–586, doi:10.1111/j.1600-0870.2008.00314.x.
- Stephenson, D. B., and I. M. Held, 1993: GCM response of northern winter stationary waves and storm tracks to increasing amounts of carbon dioxide. *J. Climate*, **6**, 1859–1870, doi:10.1175/1520-0442(1993)006<1859:GRONWS>2.0.CO;2.
- Stroeve, J. C., M. C. Serreze, M. M. Holland, J. E. Kay, J. Malanik, and A. P. Barrett, 2012: The Arctic's rapidly shrinking sea ice cover: A research synthesis. *Climatic Change*, **110**, 1005–1027, doi:10.1007/s10584-011-0101-1.
- Susskind, J., J. M. Blaisdell, and L. Iredell, 2014: Improved methodology for surface and atmospheric soundings, error estimates, and quality control procedures: The Atmospheric Infrared Sounder Science Team version-6 retrieval algorithm. *J. Appl. Remote Sens.*, **8**, 084994, doi:10.1117/1.JRS.8.084994.
- Tian-Kunze, X., L. Kaleschke, and N. Maass, 2013: SMOS daily sea ice thickness (updated 2016). ICDC, University of Hamburg, Germany, accessed January 2016. [Available online at <http://icdc.zmaw.de>.]
- Woods, C., and R. Caballero, 2016: The role of moist intrusions in winter Arctic warming and sea ice decline. *J. Climate*, **29**, 4473–4485, doi:10.1175/JCLI-D-15-0773.1.
- Zhang, J., R. Lindsay, A. Schweiger, and M. Steele, 2013: The impact of an intense summer cyclone on 2012 Arctic sea ice retreat. *Geophys. Res. Lett.*, **40**, 720–726, doi:10.1002/grl.50190.